J Mater Sci (2011) 46:4646–4653
DOI 10.1007/s10853-011-5368-0

Dielectric relaxation behavior of CdS nanoparticles and nanowires

Anoop Chandran · M. Soosen Samuel · Jiji Koshy · K. C. George

Received: 2 January 2011 / Accepted: 3 February 2011 / Published online: 15 February 2011

Abstract The dielectric relaxation and scaling behavior of CdS nanoparticles and nanowires were investigated in the frequency range 10^2–10^6 Hz and in the temperature range 373–573 K by complex impedance spectroscopy and electric modulus spectroscopy. Studies on the complex permittivity revealed that the dielectric relaxation in CdS nanostructures deviates from Debye like behavior. A detailed study on the grain and grain boundary charge transport was carried out. The charge carrier transport in CdS nanostructures was identified to be hopping of polarons. From the combined analysis of the variation of imaginary part of electric modulus and complex impedance with frequency, it was found that at high temperatures localized conduction is dominant in CdS nanoparticles where as the long range hopping process is dominant with nanowires. It was also found that the scaling behavior of CdS nanoparticles varied considerably from that reported earlier.

Introduction

Nanostructured semiconductor materials have attracted considerable attention over the past two decades due to their attractive physico-chemical properties that differ markedly from those of bulk materials. The electrical transport and dielectric properties of nanostructured materials differ from their bulk counterparts due to their large surface to volume ratio which results in the generation of large density of defects near the grain boundary [1–3]. As a result the charge carrier transport across the grain boundary is enhanced. Moreover, the space charge polarization occurring at the interfaces of the nanostructures will influence their dielectric properties [1]. In general, for nanomaterials, the grain boundaries play a significant role in the electrical and dielectric properties.

Cadmium sulfide is a direct bandgap semiconductor with a bandgap of 2.41 eV. It is a promising material for photoelectric conversion in solar cells and light-emitting diodes in flat-panel displays [4]. The CdS nanocrystals have a large number of surface located native defects such as sulfur vacancies, cadmium vacancies etc., which can act as electron/hole traps. A hole migrating to the surface of CdS can form S^- traps which were shown to be located about 1.5 eV above the valance band. For Cd^{2+} rich surfaces, the electrons are trapped in V^{2+} defect (anion vacancy) to form V^+ defect. This defect level is located about 0.7 eV below the conduction band of CdS clusters. The red emission from CdS nanoparticles have been attributed to these states [5–7]. Such trapped states, on the application of a field, lead to space charge polarization.

Due to their significance in the field of optoelectronics, various properties of CdS have been investigated by researchers. Although many studies have been carried out on the dielectric properties of CdS nanoparticles, no sufficient efforts were made to understand the exact nature of charge transport and dielectric relaxation process in them [8, 9]. Moreover, no comparative studies on the dielectric properties of CdS nanowires and nanoparticles are reported so far. In this article, we investigate in detail the dielectric relaxation and scaling behavior of CdS nanoparticles and nanowires via impedance spectroscopy and dielectric modulus spectroscopy.

A. Chandran · M. S. Samuel · J. Koshy · K. C. George (✉)
Department of Physics, S. B. College, Changanassery, Kerala 686101, India
e-mail: drkcgeorge@gmail.com

Experimental

Cadmium sulfide nanoparticles were prepared through chemical precipitation method. Reagent grade $Cd(NO_3)_2 \cdot 2H_2O$ and $(NH_2)_2 \cdot CS$ were mixed in 1:3 molar ratios (0.1:0.3 M) along with ethylenediamine using a magnetic stirrer and simultaneously heated at 90 °C for 6 h. The products were then washed with ethanol and water and dried at 100 °C for 4 h. For preparing the nanowires, the same solutions were taken in a stainless steel autoclave and placed in a preheated oven at 160 °C for 8 h. The products were then washed and dried exactly in the same way as we did for CdS nanoparticles.

The XRD analyses of the samples were performed using Bruker AXS D8 Advance X-ray diffractometer. The SEM images were taken using JEOL Model JSM-6390LV scanning electron microscope. For the dielectric studies, the as-prepared nanoparticles and nanowires of CdS were converted to pellets of 10 mm diameter and 1.1 mm thickness by applying a pressure of 4 tons for 3 min using a hydraulic press. The pellets were then placed in a tube furnace for taking measurements at various temperatures. Parameters such as complex impedance, loss tangent, electrical conductance etc. of CdS nanoparticles and nanowires were measured using HIOKI 3532-50 LCR meter. Silver electrodes were used to connect the instrument to the sample.

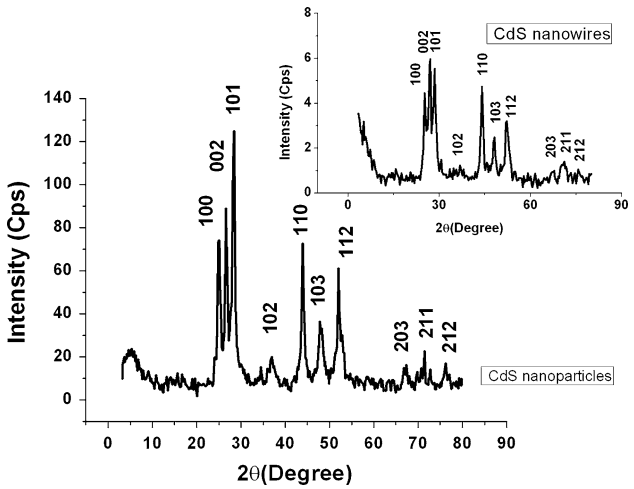

Fig. 1 The XRD pattern of CdS nanoparticles. In the *inset* is the XRD of CdS nanowires

Results and discussions

Figure 1 shows the XRD pattern of the as-prepared CdS nanoparticles and nanowires. From XRD it is evident that the obtained CdS has hexagonal wurtzite phase. The average particle sizes of both nanostructures are calculated using the Scherer's equation and are found to be 9 and 20 nm, respectively. In Fig. 2 the SEM images of the CdS nanoparticles and nanowires are shown. Most of the nanoparticles have spherical shape. Some are agglomerated and the shapes could not be determined. The nanowires are about 800 nm in length and 35 nm in diameter. The particle size obtained from the SEM image is larger than that obtained from XRD linewidths. This is attributed to the fact that XRD linewidths depend on the presence of coherent domains in the sample, whereas the SEM technique does not have that requirement and measures the actual particle size [10]. In other words the Scherer's equation do not takes into account the broadening of lines due to inhomogeneous strain (caused by dislocation and point defects which divides crystallites into much smaller incoherently scattering domains) and instrumental effects. Thus, if the contributions from these factors to the line broadening are non zero, the particle size calculated using Scherer's formula will be smaller than the actual particle size.

The most important dielectric function used to describe the dielectric dispersion is the complex dielectric constant. A detailed investigation of the dielectric spectrum might shed light into the dielectric relaxation phenomena which

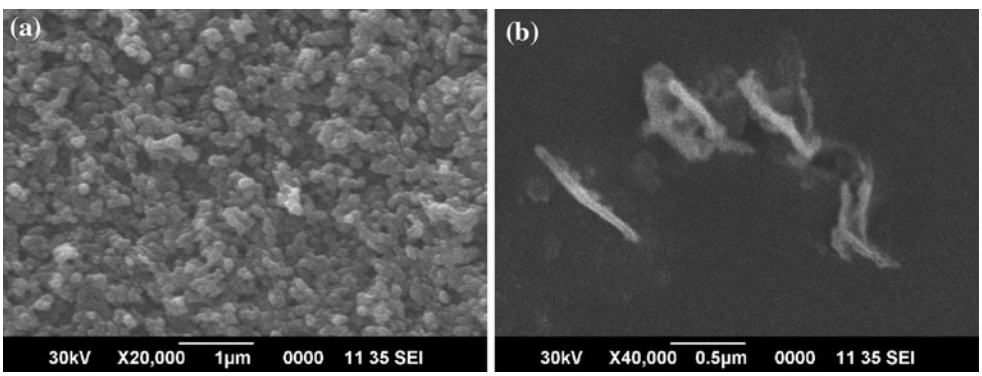

Fig. 2 The SEM images of **a** nanoparticles and **b** nanowires

takes place in dielectric materials. In CdS nanostructures, polydispersive relaxation is reported [9]. Cole–Cole plots are often used to study the relaxation behavior of such dielectrics. Following the semiempirical Cole–Cole equation [11], the real and imaginary part of the complex permittivity can be written as

$$\varepsilon'(\omega) = \varepsilon_\infty + \left(\frac{\Delta\varepsilon'}{2}\right)\left\{1 - \frac{\sinh(\beta k)}{\cosh(\beta k) + \cos\left(\beta\frac{\pi}{2}\right)}\right\} \quad (1)$$

$$\varepsilon''(\omega) = \left(\frac{\Delta\varepsilon'}{2}\right)\left\{\frac{\sin\left(\beta\frac{\pi}{2}\right)}{\cosh(\beta k) + \cos\left(\beta\frac{\pi}{2}\right)}\right\}, \quad (2)$$

where $k = \ln(\omega\tau)$, $\Delta\varepsilon' = \varepsilon_s - \varepsilon_\infty$, ε_∞ is the dielectric permittivity at high frequency, ε_s is the static dielectric permittivity, ω is the angular frequency, τ is the mean relaxation time, and $\beta = (1 - \alpha)$, where α is a measure of the distribution of relaxation times.

Figure 3 shows the variations of the real and imaginary parts of dielectric constant with frequency at different temperatures. Relaxation phenomena in dielectric materials are associated with a frequency-dependent orientational polarization. However, in nanocrystalline materials, the space charge polarization plays a significant role. This is due to the large number of electron and hole traps at the surface of nanomaterials. At low frequencies, the permanent dipoles align themselves along the field and contribute fully to the total polarization of the dielectric. At higher frequencies, the variation in the field is too rapid for the dipoles to align themselves, so their contribution to the polarization and, hence, to the dielectric permittivity can become negligible. Therefore, the dielectric permittivity decreases with increasing frequency. The values of dielectric constant observed for CdS nanostructures are higher than those reported for bulk CdS. This is attributed to the large space charge polarization taking place at the interfaces of nanostructured materials which is almost absent in conventional CdS powder.

We have fitted the experimental values of ε'' using Eq. 2. The fits are shown as solid lines in Fig. 3. The experimental and theoretical values are found to be in good agreement. The calculated parameters are listed in Table 1.

From the obtained values of α, it is evident that the dielectric relaxation behavior of CdS nanostructures deviates well from the Debye behavior. However, it can be seen that the values of α decreases slowly with increase in temperature. This means that as the temperature increases the dielectric relaxation behavior gets closer to the Debye behavior. The dielectric relaxation time is also found to decrease with temperature, which is much expected for semiconductor materials.

The relaxation peaks at low frequencies can be obscured by conductivity loss. Hence, an investigation into the electric modulus (*M**) is conducted. The electric modulus corresponds to the relaxation of electric field in the material when electric displacement remains constant. The electric modulus can be expressed as

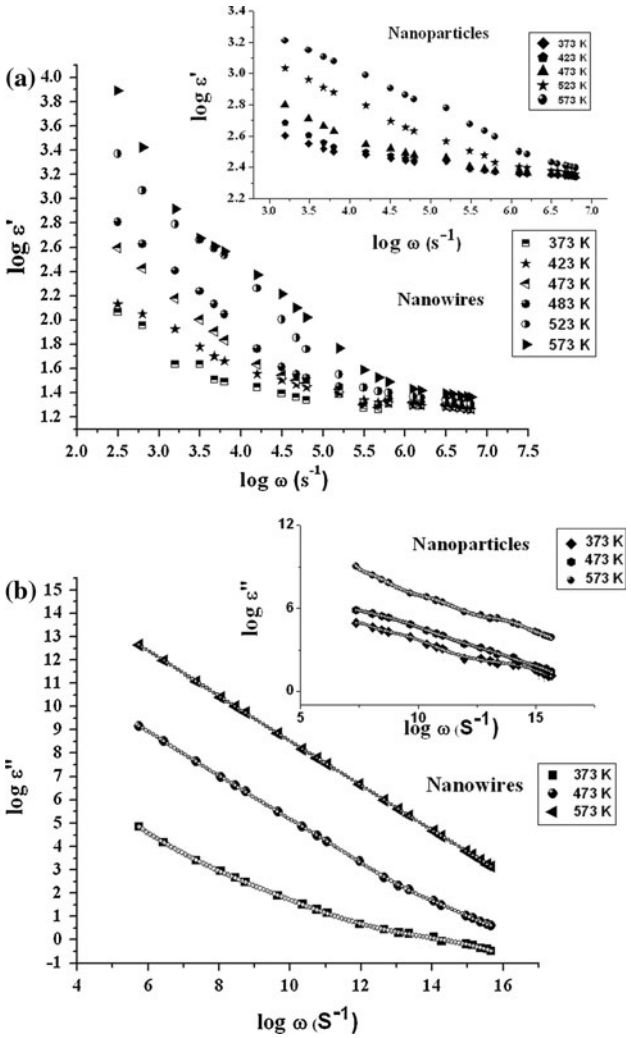

Fig. 3 The variations in the **a** real and **b** imaginary parts of dielectric constant of CdS nanowires and nanoparticles with frequency

Table 1 The parameters obtained by fitting the experimental data to Cole–Cole equation at different temperatures

	T (K)	β	α	τ (s)
CdS nanoparticles	373	0.699	0.301	0.00062
	473	0.70	0.30	0.00026
	573	0.701	0.299	0.00017
CdS nanowires	373	0.71	0.29	0.00801
	473	0.723	0.277	0.00167
	573	0.726	0.274	0.00151

$$M^*(\omega) = M' + iM'' = M_\infty \left\{ 1 - \int_0^\infty \left(\frac{\mathrm{d}\phi(t)}{\mathrm{d}t} \right) \exp(-i\omega t)\mathrm{d}t \right\}, \quad (3)$$

where M' and M'' are the real and imaginary parts of the complex modulus function, M_∞ is the asymptotic value of M' (ω), ω is the angular frequency and $\varphi(t) = \exp[-(t/\tau_M)^\xi]$ is the time evolution of the electric field within the material where ξ is the exponent and τ_M is the conductivity relaxation time [12, 13].

The electric modulus formalism is widely used to study the conductivities of dielectric materials. The study of variation of M'' with frequency provides information of the charge transport mechanism such as electrical transport and conductivity relaxation. We have plotted the real part of complex electric modulus of CdS nanoparticles and nanowires as a function of frequency in Fig. 4. From the figure it is clear that, at all temperatures, the $M'(\omega)$ values tend to zero at low frequencies and reaches a maximum value (asymptotic value) at high frequencies. Such behavior is an indicative of negligible electrode polarization phenomenon [14].

We have also plotted the imaginary part of $M^*(\omega)$ as a function of angular frequency and is shown in Fig. 5. The frequencies at which the M'' values peak follows the relation $\omega_{\max}\tau_M = 1$, where $\omega_{\max}$ is the angular frequency at which M'' shows its peak. The frequency region below the maximum peak determines the range in which charge carriers are mobile on long distances. At frequencies above $\omega_{\max}$, the carriers are confined to potential wells, being mobile on short distances. The peaks of M'' of both nanoparticles and nanowires shift to higher frequency side with increasing temperature.

The conductivity relaxation time follows the Arrhenius law given by

$$\tau_M = \tau_{M0} \exp\left(\frac{E_{\mathrm{Ma}}}{k_{\mathrm{B}}T} \right), \quad (4)$$

where τ_{M0} is the pre-exponential factor and E_{Ma} is the activation energy. The variation of conductivity relaxation time for nanoparticles and nanowires with the inverse of temperature is shown in Fig. 6. We used Eq. 4 to obtain the theoretical fit to the experimental values. The calculated activation energy and pre-exponential factor for CdS

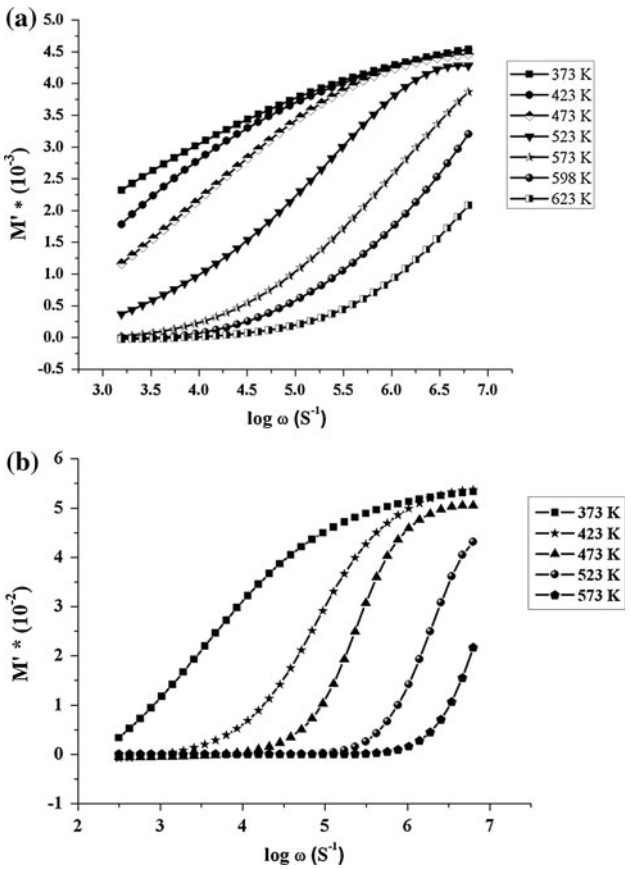

Fig. 4 Frequency dependance of the real part of electric modulus (M') of **a** CdS nanoparticles and **b** CdS nanowires

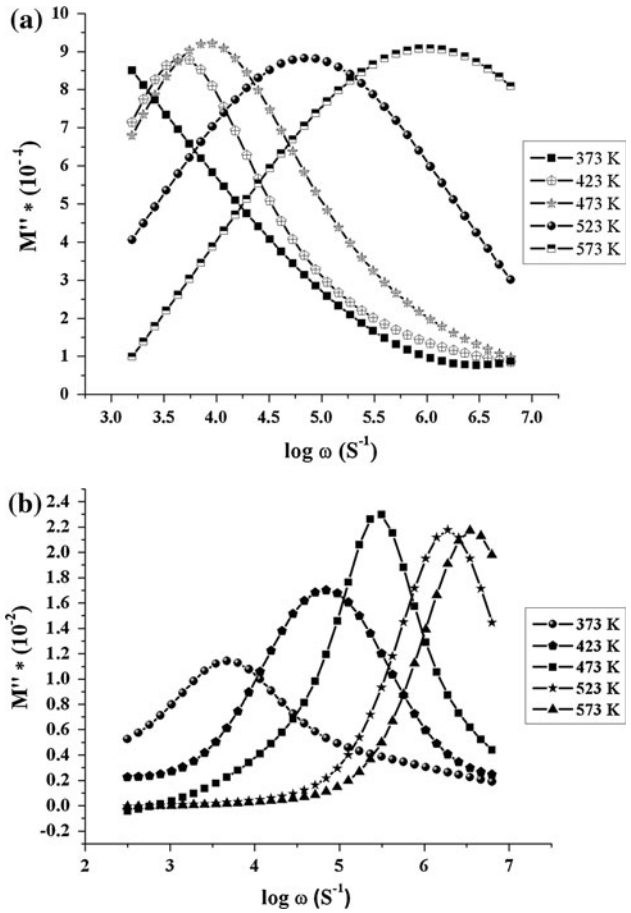

Fig. 5 Frequency dependance of the imaginary part of electric modulus (M'') of **a** CdS nanoparticles and **b** CdS nanowires

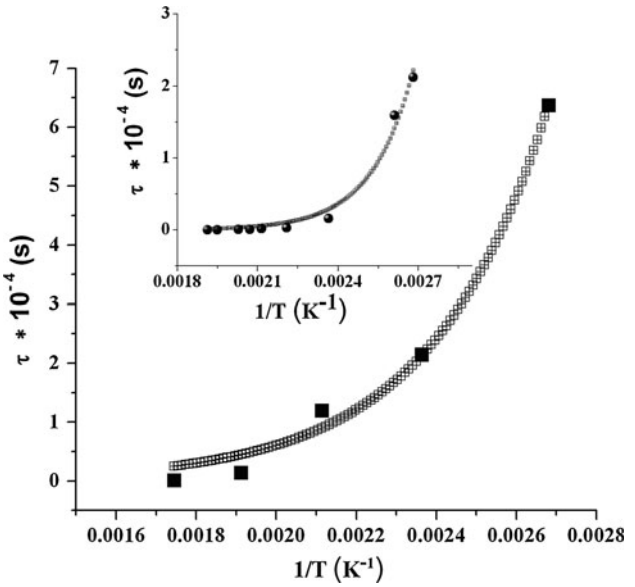

Fig. 6 The conductivity relaxation time plotted against T^{-1} for CdS nanowires and nanoparticles (*inset*)

nanoparticles are 0.299 eV and 5.87×10^{-8} s, respectively, while they are 0.557 eV and 6.63×10^{-12} s, respectively for nanowires. Such values of activation energy indicates that the conduction mechanism for CdS nanoparticles and nanowires may be due to polaron hopping based on electron carriers [15, 16]. It can be noted that the energy needed to activate hopping conduction is higher for nanowires compared to nanoparticles. This may be due to the higher density of defect centers in nanoparticles surface layers compared to that of nanowires which is a result of the high surface to volume ratio of nanoparticles.

The impedance spectrum of CdS nanoparticles and nanowires at various temperatures are shown in Fig. 7. It is obvious from the figure that only one depressed semicircle is found for CdS nanoparticles up to a temperature of 300 K. Such behavior is observed in many nanocrystalline materials and is supposed to be arising due to the overlapping of grain and grain boundary response [17, 18]. The large density of defects at the grain surface of nanostructured materials will reduce the grain boundary resistance. The smaller the particle size, the smaller is the grain boundary resistance. Hence, the time constants of grain and grain boundaries become closer in value as the particles size decreases. For CdS nanowires the appearance of the second depressed semicircle occurs at a lower temperature (473 K) compared to that of nanoparticles. This is due to the fact that nanowires have a higher grain boundary resistance than nanoparticles.

In order to obtain reliable values for the resistance of grain and grain boundary and establish a connection between microstructure and electrical properties, the equivalent

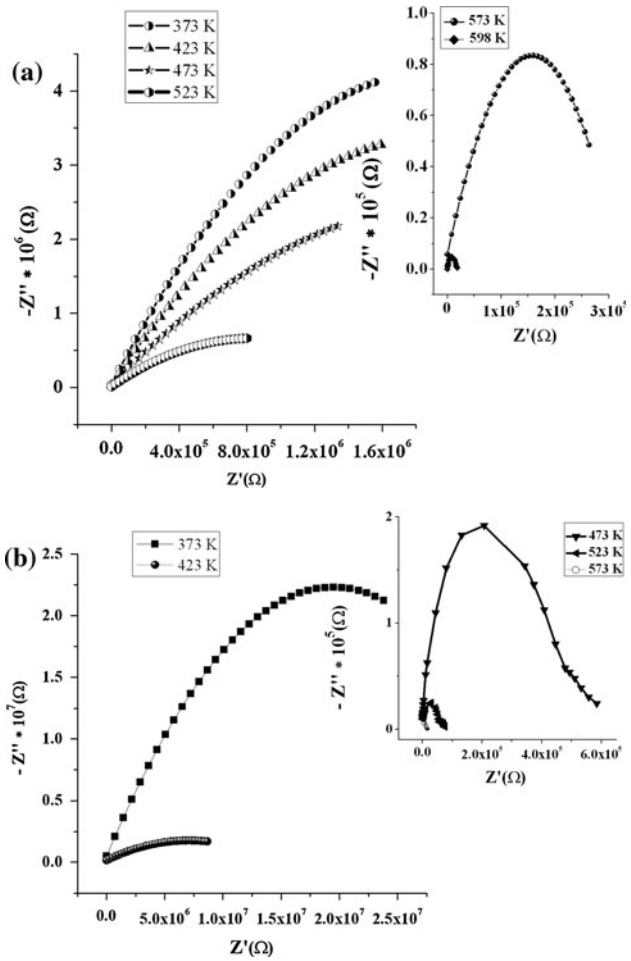

Fig. 7 The impedance spectra of **a** nanoparticles and **b** nanowires at different temperatures

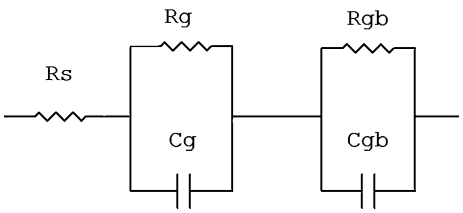

Fig. 8 The equivalent circuit model used in this study

circuit model shown in Fig. 8 is employed, which is based on the brick layer model [19]. In Fig. 8, R_s denotes the series resistance to account for the shift in the origin along the Z' axis, C_g is the capacitance related to domain and dipole reorientation in grain, R_g denotes the resistance associated with grain, C_{gb} is the capacitance related to grain boundary layer, and R_{gb} denotes the resistance across the grain boundary layer. The equivalent electrical expression for the complex impedance ($Z^* = Z' - jZ''$) can be written as

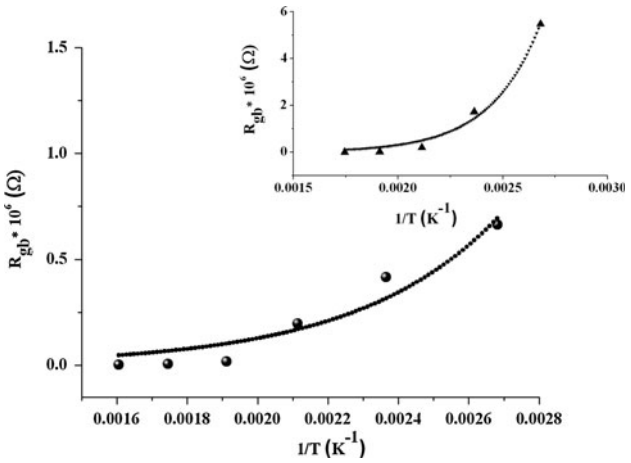

Fig. 9 The grain boundary resistance is plotted against T^{-1} for CdS nanowies and nanoparticles (*inset*)

$$Z^* = R + \frac{R_g}{1+(\omega R_g C_g)^2} + \frac{R_{gb}}{1+(\omega R_{gb} C_{gb})^2} - j\left\{ R_g\left[\frac{\omega R_g C_g}{1+(\omega R_g C_g)^2}\right] + R_{gb}\left[\frac{\omega R_{gb} C_{gb}}{1+(\omega R_{gb} C_{gb})^2}\right]\right\}. \quad (5)$$

The grain boundary and grain resistance values are calculated by fitting the obtained values by Eq. 5. It is observed that grain resistances in both nanostructures are higher than their corresponding grain boundary resistances. This is due to the large density of surface defects in these nanostructures. It is also found that the grain boundary resistance of nanowires is higher than those in nanoparticles for all temperatures. This behavior is much expected since nanoparticles have high surface to volume ratio than nanowires. The variation of R_{gb} with the inverse of temperature is shown in Fig. 9.

The resistance of the grain boundary of CdS nanostructures follows the Arrhenius law given by

$$R_{gb} = R_0 \exp\left(\frac{E_a}{k_B T}\right), \quad (6)$$

where R_0 is the pre-exponential factor and E_a is the activation energy for conduction through grain boundaries. On fitting the experimental values of R_{gb} using Eq. 6, the value of E_a obtained for nanoparticles and nanowires are 0.215 and 0.3642 eV, respectively. This makes it clear that the grain boundary conduction in nanoparticles are triggered much easily than that in nanowires, which is, once again, due to the high density of surface defects present in the former as compared to that in the latter. It should also be noticed that the activation energies obtained from electric modulus analysis is higher than those obtained for grain boundary conductivity. This is because, the electric modulus formalism takes into account both grain boundary and grain contributions in a coupled way and, hence the

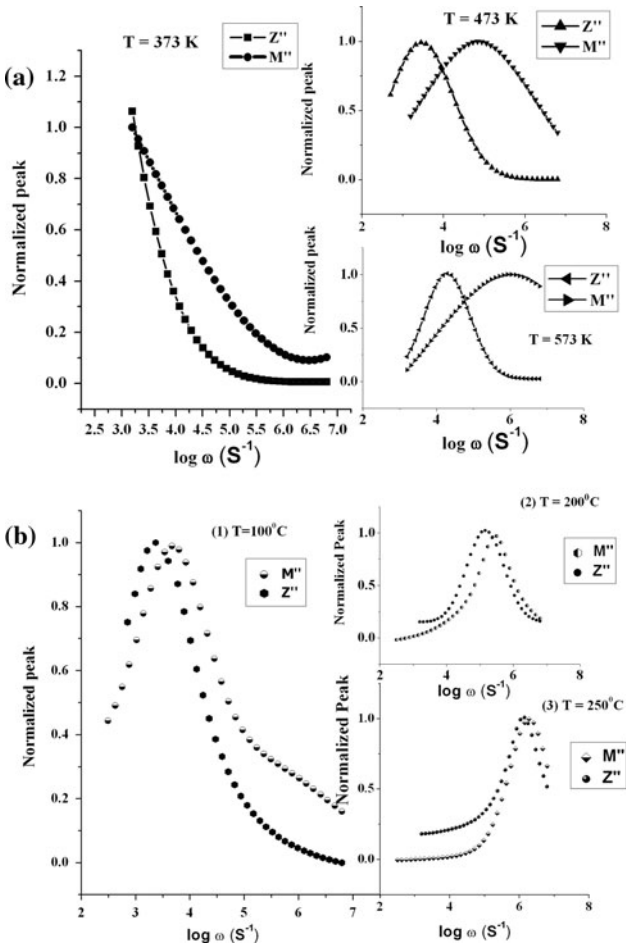

Fig. 10 Normalized imaginary parts of electric modulus and complex impedance as a function of frequency for **a** CdS nanoparicles and **b** nanowires

obtained value of activation energy represents the energy needed to activate the conduction process across both grain and grain boundary. The pre-exponential factors for nanoparticles and nanowires are found to be 869.71 and 668074 Ω, respectively.

For determining whether the short range or long range movement of charge carriers is dominant in a relaxation process, combined plots of normalized values of M'' and Z'' versus frequency can be employed. Figure 10 shows such combined plots for CdS nanoparticles and nanowires at different temperatures.

From the figure it is obvious that, for nanoparticles, there is an appreciable mismatch between normalized $Z''(\omega)$ and $M''(\omega)$ frequency dispersion curves at all temperatures. This is an evidence of localized conduction and departs from an ideal Debye behavior. In order to mobilize the localized electron, the aid of lattice oscillation is required. In these circumstances, electrons are considered not to move by themselves but by hopping motion activated by lattice oscillation, i.e., the conduction mechanism

is considered as phonon-assisted hopping of polarons between the localized states. However, for nanowires it can be seen that the peaks gets closer as the temperature rises and eventually almost overlaps at 523 K. The overlapping of the peaks is an indication of the onset of delocalized conduction [19, 20]. At this point long range hopping of electrons will become the dominant conduction mechanism.

The Cole–Cole analysis of complex dielectric constant justifies a polydispersive nature of dielectric relaxation in both CdS nanoparticles and nanowires. Nevertheless, the small variation in alpha values cannot be used to confirm whether the relaxation time is temperature dependent or not because of the uncertainties involved in fitting the data. Hence, to confirm the polydispersive nature of dielectric relaxation, we employed scaling techniques. Scaling of electric modulus can give clear information about the dependence of the relaxation dynamics on the temperature, structure and also on the concentration of the charge carriers. Therefore, we plotted the $M''(\omega, T)$ in scaled coordinates i.e., $M''(\omega, T)/M''_{\max}$ versus $\log(\omega/\omega_m)$, where ω_m is the loss peak frequency and $M''_{\max}$ is the corresponding M'' value. If all the modulus loss profiles are collapsed into one master curve, it suggests that the relaxation time is temperature independent [21]. However, it is obvious from Fig. 11 that the curves do not overlap perfectly for both nanoparticles and nanowires. At very high temperatures (above 523 K) the curves shows significant mismatch from other curves. The lack of overlap at very high temperatures suggests that the dynamic processes of charge carriers occurring at different time scales does not exhibit the same activation energy and that the distribution of the relaxation times is temperature dependent.

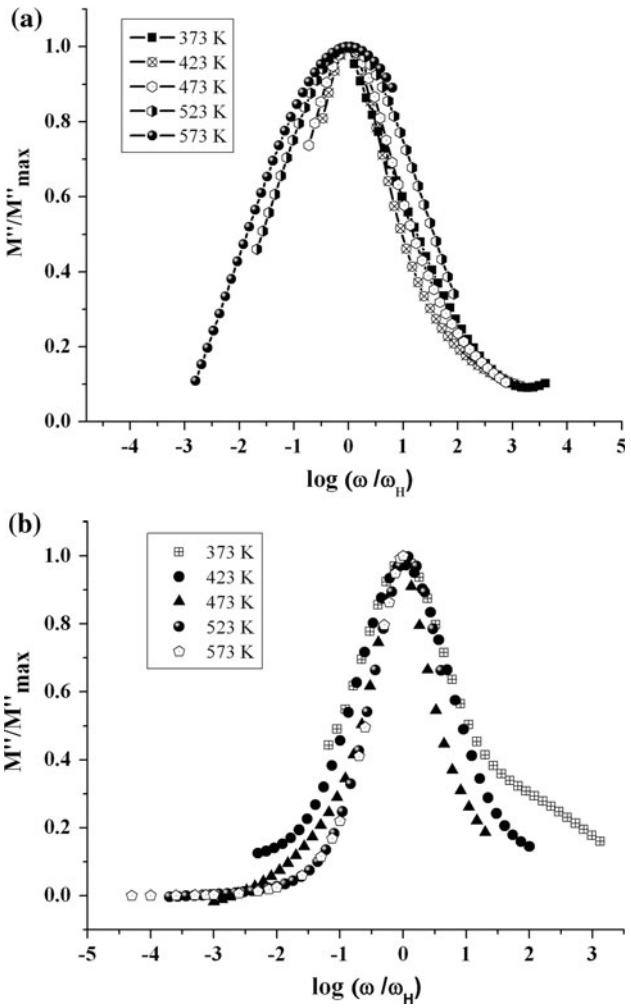

Fig. 11 The scaling behavior of M'' at different temperature for **a** CdS nanoparticles and **b** CdS nanowires

Conclusions

A detailed investigation into the relaxation and scaling behaviors of CdS nanoparticles and nanowires was made in the frequency range 10^2–10^6 Hz and in the temperature range 373–573 K. Both CdS nanoparticles and nanowires were found to exhibit Cole–Cole type relaxation. From the electric modulus spectra the conductivity relaxation time was calculated which was found to obey the Arrhenius law within the activation energy of 0.299 for nanoparticles and 0.557 for nanowires. Such high activation energy indicates the existence of polaron hopping in the material. From the analysis of impedance spectra it was found that for both nanoparticles and nanowires, the grain resistance was higher than their corresponding grain boundary resistance which is attributed to the high surface to volume ratio of these nanostructured materials. It was also found that the grain boundary resistance of CdS nanoparticles is lower than that of nanowires. This is indicative of the highly disordered surface layers of the former compared to the latter. The scaling behavior of the imaginary part of the electric modulus M'' suggested that the charge carrier transport dynamics changes at very high temperatures.

Acknowledgements The authors wish to thank Kerala State Council for Science Technology and Environment (KSCSTE) (No. (T) 012/SRS/2008/CSTE) for the financial support. The first author would like to thank STIC (Cochin) and the Common Instrumentation Facility, SB College for the analyses carried out.

References

1. Joshy J, AbdulKhadar M (2001) Mater Sci Eng A 304–306:810
2. Cassina V, Gerosa L, Podestà A, Ferrari G, Sampietro M, Fiorentini F, Mazza T, Lenardi C, Milani P (2009) Phys Rev B 79:115422
3. Biju V, Khadar MA (2003) J Mater Sci 38:4055. doi:10.1023/A:1026131103898

4. Wang C, Ao Y, Wang P, Hou J, Qian J, Zhang S (2010) Mater Lett 64:439
5. Chrysochoos J (1992) J Phys Chem 96:2868
6. Hodes G, Albu-Yaron A (1988) Proc Electrochem Soc 88–14:298
7. Jun Z, Xiao-wei D, Zhi-Iiang L, Xu G, Xing-pi Z (2007) Trans Nonferrous Met Soc China 17:1367
8. Abulkhadar M, Thomas B (1995) Phys Stat Sol A 150:755
9. Tripathi R, Kumar A, Sinha TP (2009) Pramana J Phys 72:969
10. Mukherjee S, Sudarsan V, Vatsa RK, Godbole SV, Kadam RM, Bhatta UM, Tyagi AK (2008) Nanotechnology 19:325704
11. Cole KS, Cole RH (1941) J Chem Phys 9:341
12. Macedo PB, Moynihan T, Bose R (1972) Phys Chem Glasses 13:171
13. Savitha T, Selvasekarapandian S, Ramya CS, Bhuvaneswari MS, Angelo PC (2007) J Mater Sci 42:5470. doi:10.1007/s10853-006-0983-x
14. Sural M, Ghosh A (1998) J Phys Condens Matter 10:10577
15. Dutta A, Sinha TP (2007) Phys Rev B 76:155113
16. Veena Gopalan E, Malini KA, Sakthi Kumar D, Yoshida Y, Al-Omari IA, Saravanan S, Anantharaman MR (2009) J Phy Condens Matter 21:146006
17. Chiang YM, Lavik EB, Kosacki I, Tuller HL, Ying JY (1996) Appl Phys Lett 69:185
18. Terwilliger CD, Chiang YM (1995) Acta Mater 43:319
19. Raymond O, Font R, Suárez-Almodover N, Portelles J, Siqueiros JM (2005) J App Phys 97:84108
20. Pradhan DK, Choudhary RNP, Rinaldi C, Katiyar RS (2009) J Appl Phys 106:24102
21. Baskaran N (2002) J Appl Phys 92:825